

# Crystalline and amorphous structure of astrophysical ices

G. Strazzulla

*Istituto Nazionale Astrofisica, Osservatorio Astrofisico di Catania, Catania, Italy*

E-mail: gianni@oact.inaf.it

Received September 24, 2012

The structure of water and other ices strongly depends on the temperature at which they formed, e.g., by vapor deposition. It is amorphous if ices are formed at low temperature (e.g., 10–30 K for water ice), or crystalline if the deposition temperature is higher (140–150 K). Ices have a “polycrystalline” structure at intermediate temperatures. The crystalline structure of ices can be damaged up to a complete amorphization by processes such as those due to energetic ion bombardment. Here I describe some experimental results obtained by ion irradiation of water and ammonia ices, two species particularly relevant in astrophysics. The results are discussed in the light of the relevance they have in astronomical environments where the actual structure of the ices depends on a competition between energetic processing that induce amorphization and thermal annealing that favors the transition towards more ordered structures.

PACS: 92.40.Vv Ice cores, ice sheets, ice shelves;  
61.50.Ks Crystallographic aspects of phase transformations; pressure effects;  
**61.66.-f** Structure of specific crystalline solids.

Keywords: astrophysical ice, crystalline structure, amorphous structure, ion irradiation.

## 1. Introduction

Earth based and space observations indicate that low temperature solids exist in many astrophysical environments. Condensed gases (ices) are present both in the interstellar medium as mantles on interstellar and circumstellar dust [1,2] and in/on many objects in the Solar System [3]. Ices are exposed to irradiation by energetic particles of different origins such as low energy cosmic rays, magnetospheric ions, solar flares and solar wind particles [4]. The structure (amorphous vs crystalline) of the astrophysical ices and other solids (silicates and carbons) depends on many parameters such as temperature and pressure at the time of their formation and the evolution during their long stay in space. There are several processes that drive structural changes, in particular those that induce crystalline order, as e.g. thermal annealing and those that favor damage and amorphization of the materials, as e.g. cosmic ion bombardment.

Here I present some results that have been obtained at the laboratory of experimental astrophysics (LASp) of INAF-Catania (Italy) by irradiating crystalline water or ammonia ices with energetic ions to study the induced damage and progressive (with ion flux) amorphization. Some of the data have been previously published [5,6] other data are presented here. Also described are the results obtained after irradiation of H<sub>2</sub>O:N<sub>2</sub> mixtures.

Water ice is, by far, the most abundant icy species in astrophysical environments [1,2]. Ammonia has been detect-

ed in star forming regions [7] and it is very likely to be or to have been present at the time of the formation, on the solid surfaces in the Saturnian system (e.g. Clark *et al.* 1986). In particular, the bright moons (Mimas, Enceladus, Tethys, Dione, and Rhea) could be covered by magma ejected because of tidally driven heating [8]. Recently, the first firm identification of ammonia ice that has been found in the plumes emitted by Enceladus has been reported [9].

## 2. Experimental apparatus

Experiments have been performed at the Laboratorio di Astrofisica Sperimentale of INAF-Osservatorio Astrofisico di Catania (Italy) where a stainless steel high-vacuum, recently upgraded to ultra high-vacuum ( $P < 10^{-9}$  mbar) is used. The chamber is faced to a Danfysik 200 kV ion implanter (for details see [10]). Targets are mounted at an angle of 45 degrees with respect to both the ion beam and the infrared beam of a FTIR spectrophotometer faced to the vacuum chamber. This allows to obtain “*in-situ*” spectra before and after each step of ion irradiation, without tilting or rotating the sample.

The thicknesses of the samples studied here are less than the penetration depth of the ions used (200 keV H<sup>+</sup> or 60 keV Ar<sup>++</sup>) that deposit a fraction of their energy in the ice and are stopped in the substrate (silicon or KBr). The ion current density has been maintained low enough to avoid a macroscopic heating of the samples. The spectra were taken with a resolution of 1 cm<sup>-1</sup>.

Water and or ammonia vapors were deposited at such a temperature (150 and 90 K respectively) that their structure is crystalline. The samples then have been cooled down to the chosen low  $T$  (16–80 K). At these temperatures they preserve crystalline structure and are irradiated to study the amorphization process. We use the FTIR techniques because the band profiles are very sensitive to the structure of the species.

Mixtures  $\text{H}_2\text{O}:\text{N}_2 = 1:1$ , deposited at 20 K, have an amorphous and porous structure. They have been irradiated to study the induced chemistry and the expected “compaction” of ice.

Fast ions penetrating solids deposit energy in the target by elastic and inelastic interactions that cause the breaking of molecular bonds. This produces physico-chemical modifications, erosion of material from the target and damage to the structure of the irradiated targets [4,10–12]. The energy released in the sample by impinging ions (dose) is given in eV/16u since this is a convenient way to characterize chemical changes and compare the results obtained when irradiating different samples [13].

### 3. Results

In Fig. 1, the IR spectra of water ice in the range 8000–4000  $\text{cm}^{-1}$  (1.25–2.5  $\mu\text{m}$ ) at 80 K are shown. The three spectra, shifted for clarity, refer to (from top to bottom) amorphous ice, crystalline ice and irradiated (200 keV  $\text{H}^+$ ) crystalline ice at a dose of 3.2 eV/16u. A few facts are clear from the figure: (a) both the peak position and the profile of the crystalline water ice bands are different from those of amorphous water ice; (b) particularly important is the appearance, in the crystalline ice, of a band centered at about 6050  $\text{cm}^{-1}$  (1.65  $\mu\text{m}$ ); (c) upon irradiation crystalline water ice becomes progressively amorphous.

The variation of the ratio of the area of the band at 6050  $\text{cm}^{-1}$  (1.65  $\mu\text{m}$ ) to that of the band at 6660  $\text{cm}^{-1}$

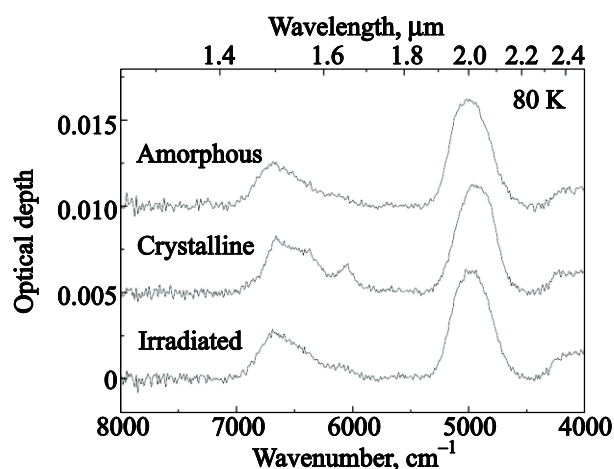


Fig. 1. IR spectra of water ice in the range 8000–4000  $\text{cm}^{-1}$  (1.25–2.5  $\mu\text{m}$ ) at 80 K. The three spectra, shifted for clarity, refer to (from top to bottom) amorphous ice, crystalline ice and irradiated crystalline ice (200 keV  $\text{H}^+$ ) at a dose of 3.2 eV/16u.

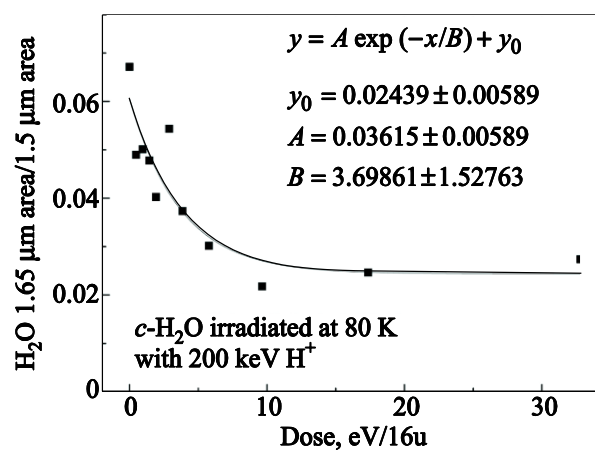


Fig. 2. The ratio of the area of the band at 6050  $\text{cm}^{-1}$  (1.65  $\mu\text{m}$ ) to that of the band at 6660  $\text{cm}^{-1}$  (1.5  $\mu\text{m}$ ) is plotted versus the dose released by 200 keV protons irradiating a crystalline water ice film at 80 K. The solid line is an exponential fit shown in the inset.

(1.5  $\mu\text{m}$ ) is a good indicator of the effects induced by bombarding. In Fig. 2 this ratio is shown versus the dose released by 200 keV protons irradiating a crystalline water ice film at 80 K. Data points have been fitted by an exponential law as shown in the Figure. A progressive, with increasing dose, transition towards an amorphous phase is evident.

In Fig. 3, IR spectra of water ice in the range 3800–2800  $\text{cm}^{-1}$  (2.63–3.57  $\mu\text{m}$ ) at 80 K are shown. The spectra refer to the as prepared crystalline ice, to the same sample irradiated (200 keV  $\text{H}^+$ ) at different doses (up to of 3.2 eV/16u). The spectrum of an amorphous sample of the same thickness is also shown for comparison.

Also for this band, due to the O–H stretching modes, the peak position and the profile of the crystalline water ice

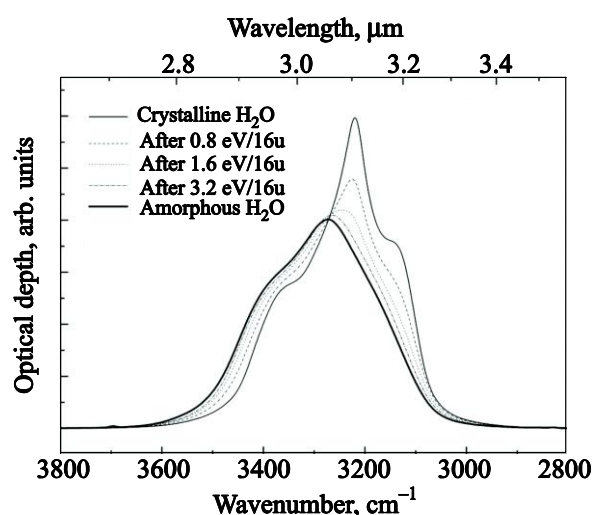


Fig. 3. IR spectra of water ice in the range 3800–2800  $\text{cm}^{-1}$  (2.63–3.57  $\mu\text{m}$ ) at 80 K. The spectra refer to the as prepared crystalline ice, to the same sample irradiated (200 keV  $\text{H}^+$ ) at different doses (up to of 3.2 eV/16u). The spectrum of an amorphous sample of the same thickness is also shown for comparison.

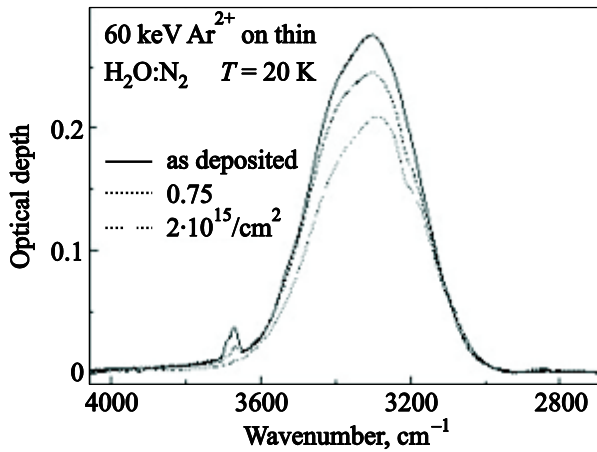


Fig. 4. IR spectra (in optical depth units) of a  $\text{H}_2\text{O}:\text{N}_2$  mixture as deposited at 20 K and after having been irradiated by 60 keV  $\text{Ar}^{2+}$ .

bands progressively changes to become almost identical to that of amorphous ice, testifying for the ion induced structural change.

One question is to understand if the amorphous structure produced by irradiation of crystalline ice is identical to that of the amorphous state obtained after gas deposition at low temperature. The answer is no, they are not identical. As deposited amorphous ice is in fact porous as evidenced by the appearance in the spectrum of the O–H dangling bond (db) bands. These bands are attributed to three- and two-coordinate water molecules [14]. The peak positions of those features vary and for pure water ice is different from those for mixtures with other species (see Table 1 in [15]). Upon irradiation, ice is compacted and those features disappear [15,16].

As a further proof of the induced compaction that testifies for the generality of the process, IR spectra (in optical depth units) of a  $\text{H}_2\text{O}:\text{N}_2$  mixture as deposited at 20 K and after having been irradiated by 60 keV  $\text{Ar}^{2+}$  are shown in Fig. 4. The spectral range is that corresponding to the stretching modes of frozen water that gives rise to the broad band. Also evident are bands at  $3672$  and  $3694\text{ cm}^{-1}$  that as said, are due to the O–H dangling bonds in porous, amorphous water ice. It is clear that in bombarded ice the db bands, which characterize frozen mixtures water/nitrogen, disappear due to the ice compaction.

The IR spectra of ammonia ice (80 K) in the range  $3600\text{--}1400\text{ cm}^{-1}$  ( $2.78\text{--}7.14\text{ }\mu\text{m}$ ) are shown in Fig. 5. The spectra refer to the as prepared crystalline ice, to the same sample irradiated with 60 keV  $\text{Ar}^{2+}$  at a dose of 33 eV/16u. The spectrum of an amorphous sample is also shown for comparison. In this case the conversion of the original crystalline structure to an amorphous one is evident.

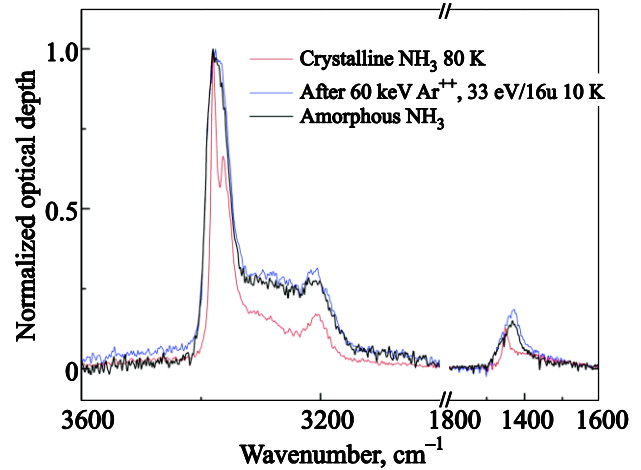


Fig. 5. IR spectra of ammonia ice in the range  $3600\text{--}1400\text{ cm}^{-1}$  ( $2.78\text{--}7.14\text{ }\mu\text{m}$ ) at 80 K. The spectra refer to the as prepared crystalline ice and to the same sample irradiated (60 keV  $\text{Ar}^{2+}$ ) at a dose of 33 eV/16u. The spectrum of an amorphous sample is also shown for comparison.

#### 4. Discussion

IR spectroscopy is a powerful technique to investigate the structure of the ices as shown above for water and ammonia ice. It is used in astrophysics to investigate the structure of ices in astrophysical environments and their evolution. The structure of the ice depends in fact on the temperature and pressure at the time of their formation, on the subsequent thermal evolution and, as discussed above, on the amount of processing (ion bombardment, but also photoprocessing, see e.g. [17]) they are exposed to.

Ice mantles of grains in dense clouds in the interstellar medium are amorphous and compact. Most likely, this reflects the fact that they are formed at low temperature by surface reaction of O (and/or  $\text{O}_2$  and/or  $\text{O}_3$ ) and H (or OH) on the cold refractory dust as experimentally evidenced [18–21]. Particularly relevant is the recent finding that molecular hydrogen reacting with OH can also produce compact amorphous ice [22].

The structure of the ice can change when clouds collapse to form young stars, which heat up their circumstellar envelopes. Under such circumstances a transition to a crystalline structure (or to evaporation when the temperature increases further) is expected [23]. At the same time, particle and photon fluxes increase and this also favors amorphization of the crystalline ices. Such a scenario has been recently observationally evidenced [24]. These authors observed a *T* Tauri star (YLW 16 A in the  $\rho$  Ophiuchi molecular cloud) and showed that crystallinity increases in the upper layers of the circumstellar disk, while only amorphous grains exist in the bipolar envelope. This implies that water ice crystallizes and remains crystallized close to the disk atmosphere where it is shielded against hard irradiation.

The competition between crystallization and amorphization also occurs on some objects in the Solar System (see e.g. [3]). In fact, ices on the surfaces of the moons in the external solar system exhibit a variety of structures [25]. The three major Jovian icy moons exhibit different structures: ice is mostly amorphous on the superficial layers of Europa (where the temperature is lower and ion fluxes are high) and crystalline on Callisto (that has the highest temperature), while both structures are found on Ganymede [26]. Roughly, the distribution of crystalline and amorphous surface ice on Ganymede is consistent with the expected distribution of energetic magnetospheric ions and neutrals, although there are not yet enough spatially resolved data to confirm the relation between the local fluxes of energetic particles and the structure of the ice.

In conclusion, I believe that laboratory data like those I discussed here are of the great relevance for understanding how astronomical observations can be used to reconstruct the evolution of ices in many astronomical environments.

### Acknowledgements

This research has been partially supported by the European COST Action CM 0805: The chemical cosmos: Understanding Chemistry in Astronomical Environments. The experimental work in Catania has been performed in the last years by the Laboratorio di Astrofisica SPERimentale (LASP) team and co-workers (G.A. Baratta, R. Brunetto, R. DiBenedetto, D. Fulvio, M. Garozzo, V. Greco, S. Ioppolo, F. Islam, Z. Kanuchova, G. Leto, M.E. Palumbo, I. Sangiorgio, F. Spinella, G. Strazzulla *et al.*).

1. E.L. Gibb, D.C.B. Whittet, A.C.A. Boogert, and A.G.G.M. Tielens, *ApJ* **151**, 35 (2004).
2. L.A. Allamandola, M.P. Bernstein, S.A. Sandford, and R.L. Walker, *SSRev.* **90**, 219 (1999).
3. J.B. Dalton, D.P. Cruikshank, K. Stephan, T.B. McCord, A. Coustenis, R.W. Carlson, and A. Coradini, *SSRev.* **153**, 113 (2010).
4. G. Strazzulla, *NIMB* **269**, 842 (2011).
5. G.A. Baratta, F. Spinella, G. Leto, G. Strazzulla, and G. Foti, *A&A* **252**, 421 (1991).
6. G. Leto, O. Gomis, and G. Strazzulla, *Mem. SAIS* **6**, 57 (2005).
7. K.I. Öberg, A.C.A. Boogert, K.M. Pontoppidan, S. van den Broek, E.W. van Dishoeck, S. Bottinelli, G.A. Blake, and N.J.II Evans, *ApJ* **740**, id. 109 (2011).
8. K. Multhaup and T. Spohn, *Icarus* **186**, 420 (2007).
9. J.H. JrWaite, W.S. Lewis, B.A. Magee, J.H. Waite, Jr., W.S. Lewis, B.A. Magee, J.I. Lunine, W.B. McKinnon, C.R. Glein, O. Mousis, D.T. Young, T. Brockwell, J. Westlake, M.-J. Nguyen, B.D. Teolis, H.B. Niemann, R.L. McNutt, Jr., M. Perry, and W.-H. Ip, *Nature* **460**, 487 (2009).
10. G. Strazzulla, G.A. Baratta, and M.E. Palumbo, *Spectrochim. Acta A* **57**, 825 (2001).
11. R.A. Baragiola, R.A. Vidal, W. Svendsen, J. Schou, M. Shi, D.A. Bahr, and C.L. Atteberry, *NIMB* **209**, 294 (2003).
12. R.E. Johnson, R.w. Carlson, J.F. Cooper, C. Paranicas, M.H. Moore, and M.C. Wong, in: *Jupiter: Planet, Satellites, and Magnetosphere*, F. Bagenal, W. McKinnon, and T. Dowling (eds.), Cambridge Univ. Press, UK, 485 (2004), p. 485.
13. G. Strazzulla and R.E. Johnson, in: *Comets in the post-Halley Era*, R.L. Newburn, Jr., M. Neugebauer, and J. Rahe (eds.), Kluwer, Publ. Co., London, 243 (1991), p. 243.
14. B. Rowland, M. Fisher, and J.P. Devlin, *J Chem. Phys.* **95**, 1378 (1991).
15. M.E. Palumbo, *A&A* **453**, 903 (2006).
16. U. Raut, M. Famá, M.J. Loeffler, and R.A. Baragiola, *ApJ* **687**, 1070 (2008).
17. G. Leto and G.A. Baratta, *A&A* **397**, 7 (2003).
18. S. Ioppolo, H.M. Cuppen, C. Romanzin, E.F. van Dishoeck, and H. Linnartz, *ApJ* **686**, 1474 (2008).
19. Y. Oba, N. Miyauchi, H. Hidaka, T. Chigai, N. Watanabe, and A. Kouchi, *ApJ* **701**, 464 (2009).
20. H. Mokrane, H. Chaabouni, M. Accolla, E. Congiu, F. Dulieu, M. Chehrouri, and J.L. Lemaire, *ApJ* **705**, L195 (2009).
21. F. Dulieu, L. Amiaud, E. Congiu, J.-H. Fillion, E. Matar, A. Momeni, V. Pirronello, and J.L. Lemaire, *A&A* **512**, id. A30 (2010).
22. Y. Oba, N. Watanabe, T. Hama, K. Kuwahata, H. Hidaka, and A. Kouchi, *ApJ* **749**, id. 67 (2012).
23. E. Dartois and L. D'Hendecourt, *A&A* **365**, 144 (2001).
24. A.A. Schegerer and S. Wolf, *A&A* **517**, A87 (2010).
25. W.M. Grundy, M.W. Buie, J.A. Stansberry, J.R. Spencer, and B. Schmitt, *Icarus* **142**, 536 (1999).
26. G.B. Hansen and T.B. McCord, *Proc. J. Geophys. Res.* **109**, E01012 (2004).